Inorganic Chemistry

Communication

pubs.acs.org/IC

$LiPbSb_3S_6$: A Semiconducting Sulfosalt with Very Low Thermal Conductivity

Eva C. Agha,[†] Christos D. Malliakas,[†] Jino Im,[‡] Hosub Jin,[‡] Li-Dong Zhao,[†] Arthur J. Freeman,[‡] and Mercouri G. Kanatzidis*,[†]

[†]Department of Chemistry and [‡]Department of Physics and Astronomy, Northwestern University, Evanston, Illinois 60208, United States

Supporting Information

ABSTRACT: The new semiconductor $LiPbSb_3S_6$ crystallizes in the space group $P2_1/c$. The structure is a member of the lillianite homologous series and is composed of layers of PbS archetype Sb/Li−S separated by trigonal-prismatic-coordinated Pb/Li. Electronic band structure calculations indicate an indirect band gap, with direct gaps lying very close in energy. $LiPbSb_3S_6$ has one of the lowest thermal conductivities seen in a crystalline material, ∼0.24 W m^{-1} K^{-1} at room temperature, and a high resistivity, ∼4 × 10^9 Ω·cm, and exhibits strong light absorption with a nearly direct band gap of 1.6 eV.

Metal chalcogenides make a broad set of structurally and chemically diverse compounds, associated with a wide range of applications including photovoltaics, thermoelectrics, second-harmonic generation, optical data storage, and γ-ray detection.[1−10] Compounds containing chalcometallate anions have shown a wide diversity ranging from discrete molecular species such as $[AsS_3]^{3-}$, $[SbS_3]^{3-}$, and $[Sb_2S_5]^{4-}$ to polymeric chains.[11−13] Particularly, ternary chalcoantimonates exhibit a surprising variety of structures because the stereochemical effect of the lone pair of the antimony ion, Sb^{3+}, gives rise to three-, four-, or five-coordination.[2,14−17] More complex structures can also result by linking the chalcoantimonate anions.[2,12,18,19] Many of these compounds absorb in the visible and IR regions, making them promising for use in photovoltaics, which ideally have direct band gaps in the optimal 1.1−1.7 eV range.[20] Ternary antimony chalcogenides, such as $AgSbTe_2$ or the series $AgPb_mSbTe_{m+2}$, have been shown to have low thermal conductivity because of strong anharmonicity and random Ag/Sb disorder, making materials of this series promising for thermoelectric applications.[21,22]

Herein we describe the new thioantimonate $LiPbSb_3S_6$, a semiconductor with an attractive band gap of 1.6 eV, high resistivity, and surprisingly low thermal conductivity. The air-stable $LiPbSb_3S_6$ was prepared by direct reaction of Li_2S, Pb, Sb, and S at 800 °C, resulting in a black crystalline material of >99% purity.[23] The crystal structure was determined with single-crystal X-ray diffraction analysis. Differential thermal analysis (DTA) shows that $LiPbSb_3S_6$ melts congruently at 576 °C (Figure 1a). The material recrystallizes in the same phase, as indicated by the full recovery of the compound from the solidified melt (Figure 1b).

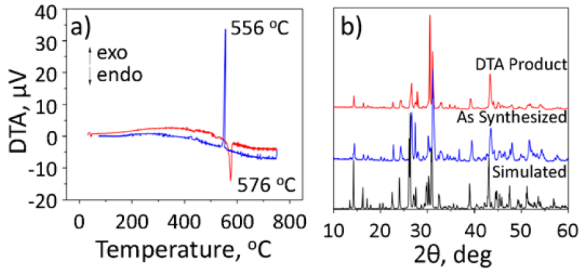

Figure 1. (a) DTA measured at ±5 °C min^{-1} shows $LiPbSb_3S_6$ to be congruently melting. (b) Powder X-ray diffraction of simulated (black), as-synthesized (blue), and DTA products (red) of $LiPbSb_3S_6$.

$LiPbSb_3S_6$ crystallizes in the monoclinic space group $P2_1/c$ with a slight off-stoichiometry of $Li_{0.97(1)}Pb_{0.91(1)}Sb_{3.068(6)}S_6$.[24] Semiquantitative elemental analysis of Pb, Sb, and S was performed by electron-dispersive spectroscopy, and qualitative X-ray photoelectron spectroscopy confirmed the presence of all elements, including Li (see the Supporting Information, SI). The structure is an analogue of the naturally occurring mineral sulfosalt gustavite, ideally $AgPbBi_3S_6$, a member of the lillianite homologous series.[25] The lillanite homologous series consists of a group of Pb−Bi−Ag sulfosalts with structures based on alternating layers of the PbS (NaCl) archetype cut parallel to $(311)_{PbS}$. Bicapped trigonal prisms of PbS_{6+2} substitute the overlapping MS_6 octehedra of these mirror-related layers, with the Pb atoms positioned on the mirror planes.[26−28] The homologues in the series differ in the width of the octahedral slabs expressed by the number of metal sites (N) in the chain that runs diagonally across an individual PbS archetypical layer and parallel to $[011]_{PbS}$.

The structure of $LiPbSb_3S_6$ consists of 11 crystallographically independent sites (Figure 2a). There are six S positions and five metal positions, which include one 100% Sb site (M3), three mixed Sb/Li sites (M2 and M5 are 95.5% Sb; M4 is 83.2% Li), and one partially unoccupied, mixed Pb/Li site (M1 is 91.1% Pb and 0.43% Li). The structure is built of alternating PbS-type slabs of Li/Sb−S cut parallel to $(311)_{PbS}$, where each layer is N = 4 octahedra thick and the slabs are separated by Pb/Li atoms in bicapped trigonal-prismatic coordination (Figure 2b). The Pb/Li site of M1 is in a bicapped trigonal-prismatic coordination, and Sb and Sb/Li sites of M2−M5 are all in distorted octahedral

Received: September 9, 2013
Published: January 9, 2014

   dx.doi.org/10.1021/ic402262z | Inorg. Chem. 2014, 53, 673−675

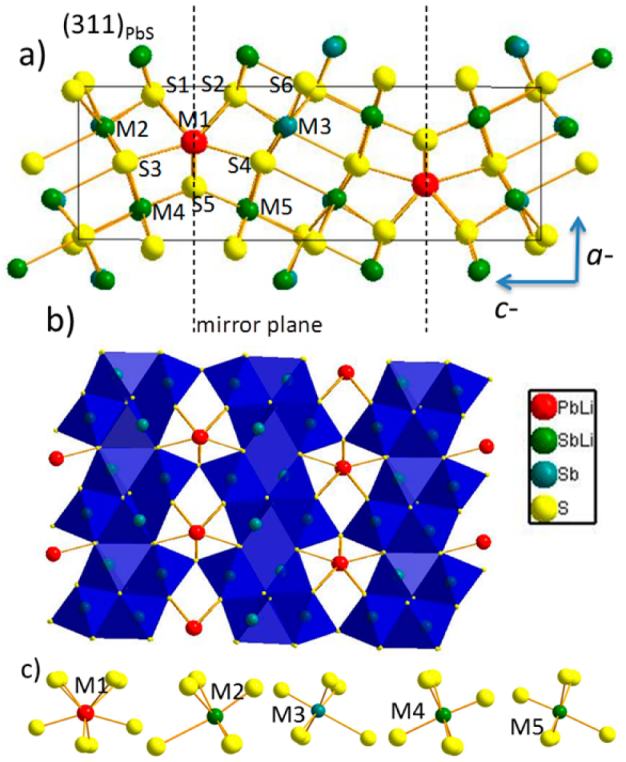

Figure 2. (a) Crystal structure of $LiPbSb_3S_6$ viewed along the *c* axis. M1 is Pb/Li (Pb is the major component) in a bicapped trigonal-prismatic coordination with coordination number 8. M2 is Sb/Li (Sb is the major component), M3 is Sb, M4 is Sb/Li (Li is the major component), and M5 is Sb/Li (Sb is the major component), all in octahedral coordination with coordination number 6. (b) Arrangement of the parallel layers of diagonal chains of four octahedra viewed along the *c* axis. Neighboring blocks of octahedral layers are separated by Pb atoms in trigonal-prismatic coordination. (c) Coordination environment of each metal site of $LiPbSb_3S_6$ viewed along the *c* axis. M1 is in a bicapped trigonal prism with coordination number 8, and M2–M5 are all in distorted octahedral coordination with coordination number 6.

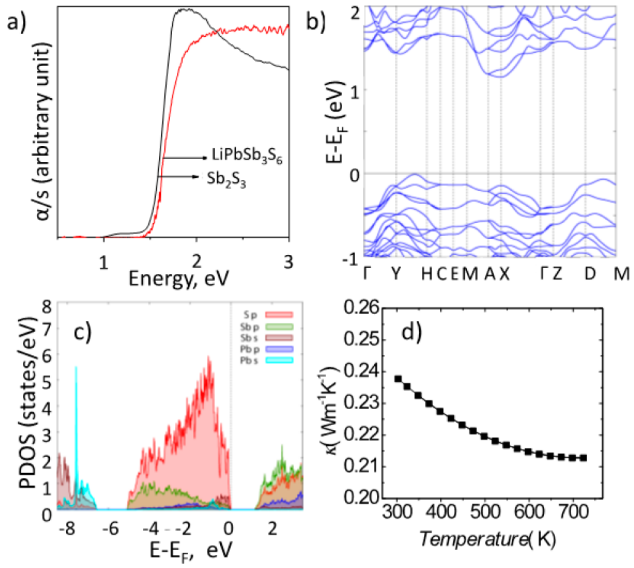

Figure 3. (a) Solid-state UV–vis optical absorption spectra for $LiPbSb_3S_6$, E_g = 1.60 eV, and Sb_2S_3, E_g = 1.55 eV. (b) Calculated band structure of $LiPbSb_3S_6$. (c) PDOS for $LiPbSb_3S_6$ comparing individual orbital contributions to the valence and conduction bands. (c) Thermal conductivity as a function of the temperature for an SPS-processed polycrystalline sample of $LiPbSb_3S_6$.

coordination (Figure 2c). The average M–S bond length is dependent on the dominant metal, with M2, M3, and M5 having longer average bond lengths than Li-dominant M4 (see the SI). This type of disorder associated with the Li ions has not been reported in $AgPbBi_3S_6$ because the structures have been determined in their idealized compositional form using the substitution 2Pb = Bi + Ag from $Pb_3Bi_2S_6$, giving a single Ag site, a single Pb site, and three Bi sites. Sb/Bi substitution is seen in some cases, such as with $AgPb(Bi_2Sb)_3S_6$, where there is mixed Sb/Bi occupancy in two of the Bi sites.[26,28]

The optical absorption properties of $LiPbSb_3S_6$ in the UV–vis/near-IR region (measured using protocols described elsewhere[29]) revealed a band gap of 1.60 eV, similar to that of Sb_2S_3, 1.55 eV. $LiPbSb_3S_6$ shows a very strong and steep absorption onset, suggestive of direct-band-gap absorption (Figure 3a). To determine the nature of the band gap of $LiPbSb_3S_6$, we performed first-principles electronic structure calculations using a generalized gradient approximation within Perdew–Burke–Ernzerhof formalism[30a] implemented in "Vienna Ab initio Simulation Package" on an idealized $LiPbSb_3S_6$ structure.[30b] The band structure (Figure 3b) is plotted along high symmetric points,[31] and density of states is projected to atomic orbitals (S p, Sb s, Sb p, Pb s, and Pb p orbitals; Figure 3c).

Electronic structure calculations show that the band gap of $LiPbSb_3S_6$ is actually indirect. The valence band maximum (VBM) is located between Y and H points, while the conduction band minimum (CBM) occurs at X. The calculated indirect band gap (E_g^i) is predicted to be 1.15 eV, and the direct band gap (E_g^d) at X point is 1.28 eV, which is only larger than E_g^i by 0.13 eV. Thus, the indirect optical transition, being spectrally forbidden, could be veiled by the much stronger allowed direct optical transition. This could explain the experimentally observed directlike transition of $LiPbSb_3S_6$. The calculated E_g^d is 0.32 eV smaller than the experimental band gap of 1.60 eV, which is consistent with the well-known tendency of these calculations to underestimate the band gap. The projected density of states (PDOS) from +3.5 to −8.5 eV, with the Fermi level at 0 eV, are shown in Figure 3c. For each atom, an orbital-resolved PDOS is shown. The major contribution to the VBM is from the S p orbitals, while the CBM mainly consists of Sb p orbitals. Thus, the band-gap transition in $LiPbSb_3S_6$ originates mainly from charge-transfer transitions from filled S to empty Sb p orbitals. The energy gap of 1.6 eV makes it interesting as a potential solar absorber for photovoltaics.

The thermal properties and resistivity of $LiPbSb_3S_6$ were measured using polycrystalline ingots, pressed using spark plasma sintering (SPS), achieving 97.8% of the theoretical density. The Seebeck coefficient was measured as $-134\ \mu V\ K^{-1}$, showing n-type behavior. The resistivity of $LiPbSb_3S_6$ is very high, at $4.24 \times 10^9\ \Omega$·cm, suggesting a relatively low number of charge carriers (see the SI).

The thermal diffusivity (D) of $LiPbSb_3S_6$ as a function of the temperature is very low and shows an inverse temperature dependence to 723 K, suggesting dominant phonon conduction behavior (see the SI). This is consistent with the insulating character of the electrical transport properties. Additionally, the heat capacity (C_p) of $LiPbSb_3S_6$ has weak, nearly linear temperature dependence (see the SI). The thermal conductivity (κ) decreases with increasing temperature from 0.24 $W\ m^{-1}\ K^{-1}$

dx.doi.org/10.1021/ic402262z | Inorg. Chem. 2014, 53, 673–675

at room temperature to 0.21 W m^{-1} K^{-1} at 723 K (Figure 3d). This decrease in the thermal conductivity with rising temperature indicates that the phonon contribution to the conductivity is predominant. The thermal conductivity of the compound is one of the lowest reported from crystalline materials. It is significantly lower than that of the exceptional thermoelectric material $Bi_xSb_{2-x}Te_3$, ~1.6 W m^{-1} K^{-1}, and close to those of glasses.[32,33] The thermal conductivity can be lowered in materials by the random alloying of atoms of differing atomic mass, the rattling of ions in oversized cages, or nanostructuring.[7,34] For example, in $Cs_2Hg_6S_7$ and $Ba_8Au_{16}P_{30}$ materials with large three-dimensional frameworks, Cs and Ba ions "rattle" and produce phonon dampening effects, which significantly reduce the lattice thermal conductivity to ~0.30 and 0.18 W m^{-1} K^{-1}, respectively.[35] In $AgSbTe_2$, on the other hand, Ag and Sb are randomly disordered. The extremely low thermal conductivity of $LiPbSb_3S_6$ appears to be similar in origin to $AgSbTe_2$ and likely results from the inherent Li/Sb and Li/Pb disorder in the metal sites of the structure.[21,22,36]

■ ASSOCIATED CONTENT

Ⓢ Supporting Information

Crystallographic information file (CIF), structural information tables, and experimental data (thermal diffusivity, heat capacity, and resistivity). This material is available free of charge via the Internet at http://pubs.acs.org.

■ AUTHOR INFORMATION

Corresponding Author

*E-mail: m-kanatzidis@northwestern.edu.

Author Contributions

All authors have given approval to the final version of the manuscript.

Notes

The authors declare no competing financial interest.

■ ACKNOWLEDGMENTS

Financial support from the National Science Foundation (Grant DMR-1104965) is gratefully acknowledged. Work in the Freeman group is funded by the Defense Threat Reduction Agency through Grant HDTRA1 09-1-0044.

■ REFERENCES

(1) Chung, D.-Y.; Choi, K.-S.; Iordanidis, L.; Schindler, J. L.; Brazis, P. W.; Kannewurf, C. R.; Chen, B.; Hu, S.; Uher, C.; Kanatzidis, M. G. *Chem. Mater.* **1997**, *9*, 3060.

(2) Park, S.; Kim, S. J. *J. Solid State Chem.* **2001**, *161*, 129.

(3) (a) Bera, T. K.; Jang, J. I.; Song, J.-H.; Malliakas, C. D.; Freeman, A. J.; Ketterson, J. B.; Kanatzidis, M. G. *J. Am. Chem. Soc.* **2010**, *132*, 3484. (b) Zhang, Q.; Chung, I.; Jang, J. I.; Ketterson, J. B.; Kanatzidis, M. G. *Chem. Mater.* **2008**, *21*, 12. (c) Zhang, Q.; Chung, I.; Jang, J. I.; Ketterson, J. B.; Kanatzidis, M. G. *J. Am. Chem. Soc.* **2009**, *131*, 9896.

(4) Shay, J. L.; Wernick, J. H. *Ternary chalcopyrite semiconductors: growth, electronic properties, and applications*; Pergamon Press: Oxford, U.K., 1975.

(5) Ebrahim-Zadeh, M.; Sorokina, I. T. *Mid-Infrared Coherent Sources and Applications*; Springer-Verlag London Ltd., London, 2008.

(6) Todorov, T. K.; Reuter, K. B.; Mitzi, D. B. *Adv. Mater.* **2010**, *22*, E156.

(7) Biswas, K.; He, J. Q.; Blum, I. D.; Wu, C. I.; Hogan, T. P.; Seidman, D. N.; Dravid, V. P.; Kanatzidis, M. G. *Nature* **2012**, *489*, 414.

(8) Owens, A. *J. Synchrotron Radiat.* **2006**, *13*, 143.

(9) Johnsen, S.; Peter, S. C.; Nguyen, S. L.; Song, J.-H.; Jin, H.; Freeman, A. J.; Kanatzidis, M. G. *Chem. Mater.* **2011**, *23*, 4375.

(10) Kanatzidis, M. G. *Curr. Opin. Solid State Mater. Sci.* **1997**, *2*, 139.

(11) Kanatzidis, M. G.; Sutorik, A. C. *Prog. Inorg. Chem.* **1995**, *43*, 151.

(12) Schimek, G. L.; Pennington, W. T.; Wood, P. T.; Kolis, J. W. *J. Solid State Chem.* **1996**, *123*, 277.

(13) Bera, T. K.; Jang, J. I.; Ketterson, J. B.; Kanatzidis, M. G. *J. Am. Chem. Soc.* **2009**, *131*, 75.

(14) Dittmar, G.; Schäfer, H. *Z. Anorg. Allg. Chem.* **1977**, *437*, 183.

(15) Cordier, G.; Schafer, H.; Schwidetzky, C. *Z. Naturforsch. B* **1984**, *39*, 131.

(16) Cordier, G.; Schwidetzky, C.; Schafer, H. *Rev. Chim. Miner.* **1982**, *19*, 179.

(17) McCarthy, T. J.; Kanatzidis, M. G. *Inorg. Chem.* **1994**, *33*, 1205.

(18) Wood, P. T.; Schimek, G. L.; Kolis, J. W. *Chem. Mater.* **1996**, *8*, 721.

(19) Hanko, J. A.; Kanatzidis, M. G. *J. Alloys Compd.* **1998**, *280*, 71.

(20) Landsberg, P. T.; Tonge, G. *J. Appl. Phys.* **1980**, *51*, R1.

(21) Morelli, D.; Jovovic, V.; Heremans, J. *Phys. Rev. Lett.* **2008**, *101*, 035901.

(22) Ye, L.-H.; Hoang, K.; Freeman, A.; Mahanti, S.; He, J.; Tritt, T. M.; Kanatzidis, M. *Phys. Rev. B* **2008**, *77*, 245203.

(23) McCarthy, T. J.; Kanatzidis, M. G. *Inorg. Chem.* **1995**, *34*, 1257.

(24) Crystals of $LiPbSb_3S_6$ are in the monoclinic space group $P2_1/c$ with a = 6.8964(5) Å, b = 19.7941(18) Å, c = 8.3942(6) Å, α = 90°, β = 108.038(5)°, γ = 90°, V = 1089.56(15) $Å^3$. Other crystal data: Z = 4; θ_{max}(Mo Kα) = 30.49°; total reflections, 12798; unique reflections, 3121; number of variables, 104; μ = 22.652 mm^{-1}; D_c = 4.6545 g/cm^3; R_{int} = 5.33%; GOF = 2.40; R_1 = 5.62%; R_w = 13.7% for $I > 2\sigma(I)$.

(25) Karup-Moeller, S. *Can. Mineral.* **1970**, *10*, 173.

(26) Ferraris, G.; Makovicky, E.; Merlino, S. *Crystallography of Modular Materials*; Oxford University Press: Oxford, U.K., 2004.

(27) Pring, A.; Jercher, M.; Makovicky, E. *Mineral. Mag.* **1999**, *63*, 917.

(28) Pazout, R.; Dusek, M. *Acta Crystallogr., Sect. C: Cryst. Struct. Commun.* **2009**, *65*, I77.

(29) (a) Liao, J. H.; Varotsis, C.; Kanatzidis, M. G. *Inorg. Chem.* **1993**, *32*, 2453. (b) Chondroudis, K.; McCarthy, T. J.; Kanatzidis, M. G. *Inorg. Chem.* **1996**, *35*, 840.

(30) (a) Perdew, J. P.; Burke, K.; Ernzerhof, M. *Phys. Rev. Lett.* **1996**, *77*, 3865. (b) Kresse, G.; Hafner, J. R. *Phys. Rev. B* **1993**, *47*, 558.

(31) Setyawan, W.; Curtarolo, S. *Comput. Mater. Sci.* **2010**, *49*, 299.

(32) Wachter, J.; Chrissafis, K.; Petkov, V.; Malliakas, C.; Bilc, D.; Kyratsi, T.; Paraskevopoulos, K.; Mahanti, S.; Torbrügge, T.; Eckert, H. *J. Solid State Chem.* **2007**, *180*, 420.

(33) Poudel, B.; Hao, Q.; Ma, Y.; Lan, Y. C.; Minnich, A.; Yu, B.; Yan, X. A.; Wang, D. Z.; Muto, A.; Vashaee, D.; Chen, X. Y.; Liu, J. M.; Dresselhaus, M. S.; Chen, G.; Ren, Z. F. *Science* **2008**, *320*, 634.

(34) Girard, S. N.; He, J. Q.; Zhou, X. Y.; Shoemaker, D.; Jaworski, C. M.; Uher, C.; Dravid, V. P.; Heremans, J. P.; Kanatzidis, M. G. *J. Am. Chem. Soc.* **2011**, *133*, 16588.

(35) (a) Li, H.; Peters, J. A.; Liu, Z.; Sebastian, M.; Malliakas, C. D.; Androulakis, J.; Zhao, L.; Chung, I.; Nguyen, S. L.; Johnsen, S.; Wessels, B. W.; Kanatzidis, M. G. *Cryst. Growth Des.* **2012**, *12*, 3250. (b) Fulmer, J.; Lebedev, O. I.; Roddatis, V. V.; Kaseman, D. C.; Sen, S.; Dolyniul J. A.; Lee, K.; Olenev, A. V.; Kovnir, K. *J. Am. Chem. Soc.* **2013**, *135*, 12313−12323.

(36) Geller, S.; Wernick, J. *Acta Crystallogr.* **1959**, *12*, 46.